International Journal of Pharmaceutics 496 (2015) 75–85

Contents lists available at ScienceDirect

International Journal of Pharmaceutics

journal homepage: www.elsevier.com/locate/ijpharm

# Evaluation of spin freezing versus conventional freezing as part of a continuous pharmaceutical freeze-drying concept for unit doses

L. De Meyer [a,*], P.-J. Van Bockstal [a], J. Corver [b], C. Vervaet [c], J.P. Remon [c], T. De Beer [a]

[a] Laboratory of Pharmaceutical Process Analytical Technology, Department of Pharmaceutical Analysis, Ghent University, Ottergemsesteenweg 460, B-9000 Ghent, Belgium
[b] RheaVita, High Tech Campus 9, NL 5656 AE Eindhoven, The Netherlands
[c] Laboratory of Pharmaceutical Technology, Department of Pharmaceutics, Ghent University, Ottergemsesteenweg 460, B-9000 Ghent, Belgium

ARTICLE INFO

*Article history:*
Received 9 January 2015
Received in revised form 7 May 2015
Accepted 9 May 2015
Available online 14 May 2015

*Keywords:*
Freeze-drying
Continuous freeze drying
Spin freezing
NIR spectroscopy

ABSTRACT

Spin-freezing as alternative freezing approach was evaluated as part of an innovative continuous pharmaceutical freeze-drying concept for unit doses. The aim of this paper was to compare the sublimation rate of spin-frozen vials versus traditionally frozen vials in a batch freeze-dryer, and its impact on total drying time.

Five different formulations, each having a different dry cake resistance, were tested.

After freezing, the traditionally frozen vials were placed on the shelves while the spin-frozen vials were placed in aluminum vial holders providing radial energy supply during drying. Different primary drying conditions and chamber pressures were evaluated.

After 2 h of primary drying, the amount of sublimed ice was determined in each vial. Each formulation was monitored in-line using NIR spectroscopy during drying to determine the sublimation endpoint and the influence of drying conditions upon total drying time.

For all tested formulations and applied freeze-drying conditions, there was a significant higher sublimation rate in the spin-frozen vials. This can be explained by the larger product surface and the lower importance of product resistance because of the much thinner product layers in the spin frozen vials. The in-line NIR measurements allowed evaluating the influence of applied drying conditions on the drying trajectories.



## 1. Introduction

Lyophilisation or freeze-drying is a low temperature drying process, based on principles of mass and heat transfer, employed to convert solutions of (heat) labile materials into solids having sufficient stability for distribution and storage. Pharmaceutical freeze-drying is a batch process, although the handling equipment before (filling) and after (capping and packaging) freeze-drying is continuously operated. A typical pharmaceutical freeze-dryer consists of a drying chamber in which the vials (pharmaceutical unit doses typically containing 0.5–10 ml of a solution) are placed on temperature controlled shelves (see Fig. 1). The shelf temperature is set and controlled during processing using a thermal fluid flowing through the shelves. A lyophilisation cycle consists of three consecutive steps: freezing, primary drying, and secondary drying (Pikal, 2002; Wang, 2000; Khairnar et al., 2013).

During freezing, the shelves are chilled and most of the water in the formulation crystallizes to ice, thus concentrating the solutes between the ice crystals. Some of the solutes crystallize, while those that do not are transformed into a rigid glass when the product temperature drops below the glass transition temperature (Tg') of the amorphous matrix (Kasper and Friess, 2011). At the end of the freezing step a frozen plug is formed at the bottom of the vial. Primary drying is induced by reducing the chamber pressure and increasing the shelf temperature (to supply energy for sublimation), hence removing the ice crystals by sublimation. The ice–vapor interface in the vials, i.e., the sublimation front, moves slowly downward as the sublimation process progresses. During primary drying, the product temperature is kept below the collapse temperature (Tc), hence ensuring a solid and rigid cake after lyophilisation. Freeze-drying ends with a secondary drying step under deep vacuum where most of the unfrozen water (i.e., water dissolved in the solid amorphous phase) is removed by desorption (Pikal, 2002). Since no crystalline water (ice) is present during secondary drying, it is performed at a higher shelf temperature without the risk of thawing of the product.

* Corresponding author. Tel.: +32 9 264 83 55; fax: +32 9 222 82 36.
*E-mail address:* laurens.demeyer@ugent.be (L. De Meyer).

http://dx.doi.org/10.1016/j.ijpharm.2015.05.025
0378-5173/

The drying chamber is connected to the condenser via a duct. During primary and secondary drying, the sublimated ice and removed water is captured on the condenser, where the temperature and vapor pressure are kept lower than in the drying chamber.

Freeze drying performed via this batch-wise concept has several important disadvantages:

1. The freezing step is uncontrolled at the vial level, which has significant impact on the consecutive drying steps. Freezing initially involves the cooling of all aqueous solutions (vials) in the freeze-dryer until ice nucleation occurs. The solutions generally do not freeze spontaneously at their equilibrium freezing point (0 °C). The retention of the liquid state below the equilibrium freezing point of the solution is termed as 'supercooling'. Ice nucleation is in general a stochastic event, hence inducing vial-to-vial variation based on the degree of supercooling: a higher degree of supercooling increases the rate of ice nucleation and the effective rate of freezing, yielding a high number of small ice crystals. In contrast, at a lower degree of supercooling, a lower number of large ice crystals is formed. As a consequence, the size of the ice crystals differs from vial to vial which affects the sublimation rate (i.e., required drying time) during primary drying. Example as a high degree of supercooling produces small ice crystals, smaller pores are formed in the dried layer during sublimation, which offers a higher resistance to water vapor transport during primary drying. Smaller pores will also decrease the ease of reconstitution of the freeze dried product. (Kasper and Friess, 2011).
2. Uneven heat transfer in the freeze-drying chamber. This results in differences in energy input in vials that are placed at different locations on the freeze-dryer shelves. Example vials on the edge of the shelves are exposed to more heat radiation transfer from the warmer surroundings (i.e., door and walls of the freeze-dryer) compared to the vials in the middle of the shelves. This vial-to-vial variability in heat transfer results in significant vial-to-vial difference towards product temperature (danger for collapse!) and drying rate (see Fig. 2) (Kauppinnen et al., 2013). Both, disadvantages 1 and 2 result in different freeze-drying process conditions in each vial, which might lead to uncontrolled vial-to-vial and batch-to-batch end product variability (e.g., differences in residual moisture content, API state and stability). However, quality is only assessed on a very small fraction of the vials in the freeze-dried batch prior to batch release, which might not represent the entire batch. Such a manufacturing approach is in conflict with the recent Quality-by-Design and Process Analytical Technology guidelines from the regulatory authorities (FDA and EMA), stating that quality should be built into and guaranteed in each dosage form (i.e., in each released vial) (ICH Q8(R2), 2009).
3. It is a slow, and hence time-consuming and expensive process. The whole cycle may last 1 to 7 days (and even more) depending on the product properties and the dimensions of the vials (Tang and Pikal, 2004).
4. It is a batch process. In an industrial environment large numbers (tens of thousands) of vials are treated per batch, which induces operational risks, such as complicated handling of vials for loading and unloading of the freeze-dryer. Furthermore, since the handling equipment before (filling) and after (capping, packaging) freeze drying is continuously operated by nature, buffer systems are necessary. This increases the risk of product contamination.
5. The handling equipment takes up a large area of space, which is very expensive in terms of capital investment and operational costs because of the high standards of cleanliness and sterility, which are mandatory in production of biopharmaceuticals (Baertschi et al., 2011).
6. A batch freeze-dryer is commonly designed and optimized to process only the largest applicable amount of vials. Different loadings will require different optimal process conditions in the freeze-drying chamber and may not be allowed for that reason,

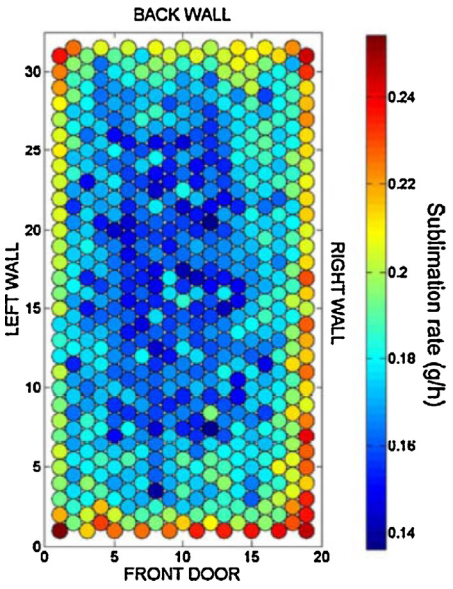


**Fig. 2.** Temperature differences of vials depending on their location on the freeze-dryer shelf (Kauppinnen et al., 2013).

**Fig. 1.** Lab-scale freeze drying chamber with four temperature controlled shelves.

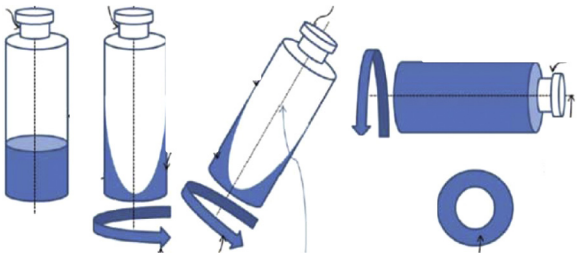

**Fig. 3.** Spin freezing of a vial.

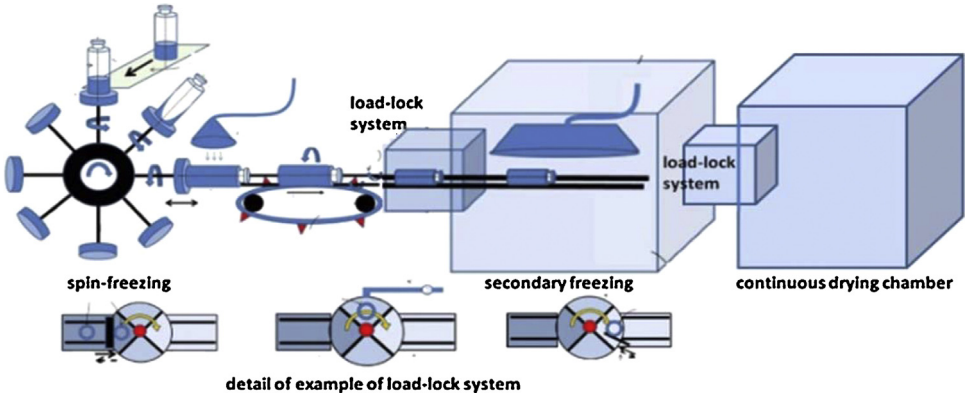


**Fig. 4.** Continuous freezing system connected to a continuous drying system.

unless separately validated. And it is possible that the required batch sizes are smaller which leads to inefficient use of the infrastructure.

7. The installation is subject to various thermal and pressure conditions. This leads to thermal inefficiencies and the transient conditions may not be well defined.
8. The course of the freeze drying process cannot be monitored at the scale of the individual vial. The product behavior (at molecular level) in each vial during freeze-drying is unknown (Kauppinnen et al., 2013).
9. Up-scaling from lab-scale freeze-dryers to pilot-scale and industrial-scale freeze-dryers requires extensive re-optimisation and re-validation of the process (Rambhatla et al., 2004; Trappler, 2004).

To overcome these disadvantages, a continuous freeze-drying concept is presented and evaluated (Corver, 2013).

## 2. Continuous pharmaceutical freeze-drying of unit doses

The continuous freeze-drying concept starts with a continuous freezing step where the vials, filled with the liquid formulation, are rotated rapidly along their longitudinal axis (i.e., spin-freezing, see Fig. 3). The cooling and freezing of the solution is achieved by using a flow of sterile gas with a controllable temperature around the rotating vial. Consequently, the resulting frozen product will be spread over a larger (i.e., entire) vial surface compared to traditional freeze-drying. The remainder of the cooling process in order to establish the desired morphological structure of the ingredients and to further crystallize and solidify the excipients and APIs under the desired process conditions will be achieved by transferring the vials to a chamber with a controlled temperature (see Fig. 4).

An appropriate load-lock system will be used to transfer the frozen vials between the continuous freezing and the continuous primary drying unit, both having different conditions of pressure and temperature (see Fig. 4). It is known from the industrial applications of vacuum deposition that the application of load-locks is required to separate chambers with different conditions to enable a continuous product flow (Ramsay, 2003). Two drying chambers (one for primary and one for secondary drying – the latter not shown in Fig. 4) will be used. In each drying chamber, an endless belt system with pockets to hold the individual vials will allow the transport of the vials and the heat transfer to the vials needed for sublimation and desorption, allowing individual vial energy input regulation. Since the frozen product is spread over the entire vial surface (resulting in thin product layers), it is important to assure adequate and uniform energy supply from the pocket to the product shell in a radial manner. This supply of energy may take place by radiation or conduction. In a conventional freeze-dryer, the sublimated ice and desorbed water is collected using cryogenic ice condensers. For this continuous freeze-drying concept, a condenser system will be used allowing to continuously remove the condensed water. By increasing the surface area of the product in the vial, and by consequently decreasing the product layer thickness, it is our estimation (as further experimentally proven) that for some pharmaceutical compositions the total process time (under optimized process conditions) may be reduced with a factor 10–40, depending of the specific formulation properties and vial dimensions. Increasing the vial throughput (i.e., scale-up) can be simply done by adding parallel lines in the continuous freeze-drying technology modules. Hence, scale-up will not require complete re-optimization and re-validation of the process because scale-up is realized by running the continuous production line for a longer period of time. Freeze-drying of exactly the required amount of vials also becomes possible.

## 3. Aim of the paper

The aim of this study is to evaluate spin freezing as part of a continuous pharmaceutical freeze-drying concept for unit doses. More specifically, the difference in sublimation rate between spin frozen vials and traditionally frozen vials in a batch freeze-dryer was evaluated and its impact on total drying time.

**Table 1**
Dry product resistance of the different used formulations (Kuu et al., 2006).

| | Formulation | $R_p$ ($cm^2$ m Torr h $g^{-1}$) |
|---|---|---|
| 1 | Trehalose: 45 mg/ml; polysorbate 20: 0.1 mg/ml; 5 mM Histidine pH 6.0 | 0.5 |
| 2 | Lactose: 30 mg/ml; sucrose: 3.42 mg/ml; glycine: 3.75 mg/ml; sodium chloride: 0.58 mg/ml | 1.067 |
| 3 | Mannitol: 30 mg/ml; sucrose: 3.42 mg/ml; glycine: 3.75 mg/ml; sodium chloride: 0.58 mg/ml | 0.3861 |
| 4 | Lactose: 30 mg/ml | 1.771 |
| 5 | Sucrose: 30 mg/ml | 1.443 |

**Fig. 5.** Aluminum vial holder.

## 4. Materials and methods

Five different formulations having a different specific dry product resistance were selected from literature (Kuu et al., 2006; Overcashier et al., 1999) (Table 1).

Trehalose was purchased from Cargill (Germany). Polysorbate 20, sodium chloride, lactose and mannitol were purchased from Fagron (Belgium). L-histidine and glycine were purchased from Sigma–Aldrich (United States).

Prior to freeze-drying, 10 ml type I glass vials were filled with a specific volume of the formulation (see Section 4.2).

After Freezing (see Section 4.1), all frozen vials were dried in an Amsco FINN-AQUA GT4 freeze-dryer (GEA, Köln, Germany).

### 4.1. Spin freezing versus traditional freezing

A specific aim of this study was to experimentally compare the sublimation rate (and drying time) of spin frozen vials to traditionally frozen vials, and to investigate the influence of drying process parameters upon sublimation rate for both types of frozen vials. Mathematical calculations and simulations of the sublimation rate and primary drying process for the five used model formulations was beyond the scope of this manuscript, but is extensively described in another submitted manuscript. This study (being part of a continuous freeze-drying system for unit doses study) aimed at experimentally exploring and demonstrating the drying differences between spin frozen and traditionally frozen vials of the five model formulations.

Prior to each freezing–drying experiment, the mass of the empty and filled vials was determined to calculate the mass of the filled volume. After each freeze-drying experiment, the mass of the vial containing the dried product was determined and the mass of sublimated water could hence be calculated.

During spin freezing, the vials were rotated (spinned) around their longitudinal axis at 2500 rotations per minute (rpm). Eq. (2) suggested that 2500 rpm resulted in an equally spread product layer with a maximal layer thickness difference of 10% between the bottom and the top of the product layer.

**Table 2**
Factors studied in experimental design.

| Factor | Level | | | | |
|---|---|---|---|---|---|
| Formulation | 1 | 2 | 3 | 4 | 5 |
| Freezing method | batch | | | spin | |
| Freezing rate | liquid nitrogen | | | dry ice | |
| Vial filling volume (ml) | 3 (1.2 mm) | | 3.5 (1.5 mm) | 4 (1.7 mm) | |
| Shelf temperature (°C) | 5 | | | 40 | |
| Chamber pressure (μbar) | 100 | | | 300 | |

**Table 3**
Full factorial design containing two factors (formulation and pressure) and one response (total drying time).

| Exp No | Formulation | Pressure (μbar) | Total drying time (min) |
|---|---|---|---|
| 1 | Formulation 1 | 100 | 152 |
| 2 | Formulation 2 | 100 | 158 |
| 3 | Formulation 3 | 100 | 175 |
| 4 | Formulation 4 | 100 | 174 |
| 5 | Formulation 5 | 100 | 153 |
| 6 | Formulation 1 | 300 | 138 |
| 7 | Formulation 2 | 300 | 139 |
| 8 | Formulation 3 | 300 | 133 |
| 9 | Formulation 4 | 300 | 152 |
| 10 | Formulation 5 | 300 | 146 |

$$\omega = \sqrt{\frac{\Delta h \times 2g}{r_1^2 \times r_2^2}} \quad (2)$$

where $\omega$ is the angular velocity (rad/sec), $\Delta h$ the height of the spin frozen product layer, g the gravitational constant and $r_1$ and $r_2$ the layer thickness at the bottom and the top respectively.

The NIR probe interface (see Section 4.3) was created in the middle of the vial, where the deviation in layer thickness was 0%. When the solution was spread over the circumferential vial wall during spinning, the vial was submerged in liquid nitrogen or surrounded by dry ice. After formation of the frozen product layer, the vials were immediately transferred to −35 °C pre-cooled aluminum vial holders in the freeze-dryer, after which vacuum was introduced and the shelf temperature set point was changed to 5 °C or 40 °C. To supply energy for sublimation through the sidewall of the spin frozen vials, the aluminum vial holders (see Fig. 5) were placed on the shelf in the freeze drier in which the vials were placed, thereby creating direct contact between the aluminum holder and the vial. The energy of the shelf was hence conducted through the aluminum vial holders to the spin frozen vials. Due to the high thermal conductivity of aluminum (205 $W\,m^{-1}\,K^{-1}$) and the close contact between the shelf and the vial holders, the temperature of the shelf and the holders was the same (as experimentally verified with thermocouples).

For the traditional frozen vials, the vials were placed vertically in liquid nitrogen or on dry ice until the solution formed a frozen plug at the bottom of the vial. Afterwards, the vials were immediately transferred to the freeze-dryer and placed on the at −35 °C pre-cooled shelves. Thereafter, the vacuum was introduced and the shelf temperature set point was changed to 5 °C or 40 °C.

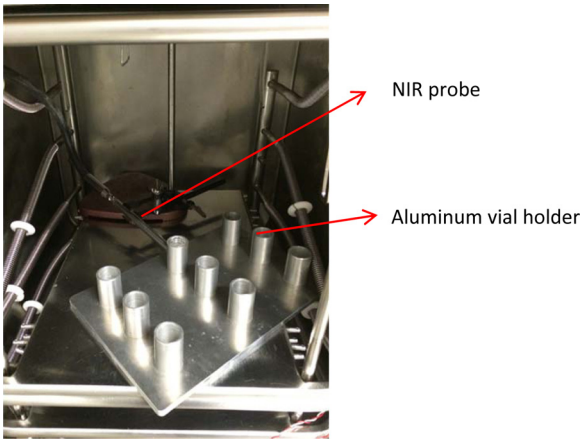


**Fig. 6.** In-line NIR monitoring experiment setup.

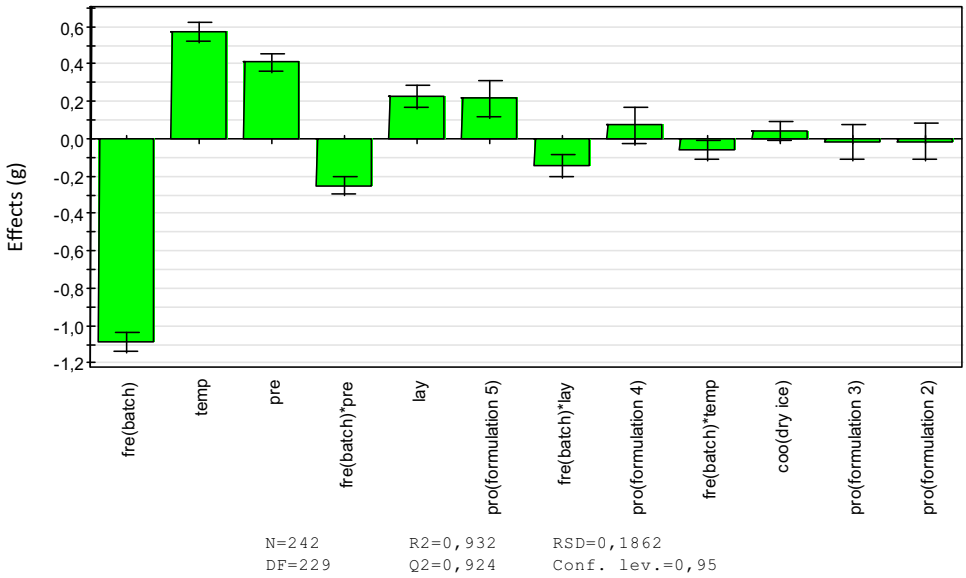


**Fig. 7.** Effect plot of the full factorial design containing all the data. Freezing method (fre), temperature (temp), chamber pressure (pre), formulation (pro), layer thickness (lay), freezing rate (coo).

The applied freeze-drying conditions varied according to an experimental design plan (see Section 4.2). When the vacuum was introduced, the primary drying shelf set point temperature was set (5 °C or 40 °C) and kept constant till the end of the experiment.

### 4.2. Design of experiments

A full factorial experimental design was performed to study the influence of five formulations having different $R_p$ values (Table 1), filling volume, freezing method and rate and drying settings upon the mass of sublimed water after 2 h of drying. An overview of these factors and their studied ranges is given in Table 2. This design, consisting of six factors (one factor with five levels, one factor with three levels and four factors with two levels), resulted in 240 experiments. Three centerpoint experiments were added, leading to 243 experiments in total.

A second full factorial design (10 experiments, see Table 3) was performed to study the influence of the five formulations and chamber pressure upon total drying time of spin-frozen vials in liquid nitrogen.

The drying endpoint was determined in-line using NIR spectroscopy. For traditionally frozen vials (having rather thick product layers, >0.5 cm), the drying endpoint of different formulations was for an important part influenced by their dry product resistance ($R_p$). For spin frozen formulations having different $R_p$ values, the drying endpoint was expected to be similar because of the thin product layers. When having optimal direct contact between the vial and the vial holder (see Section 4.1), the chamber pressure was expected not to influence the sublimation rate. However, this contact in our experimental setup was not perfect. Therefore, the influence of chamber pressure upon the total drying time of the spin frozen formulations was also

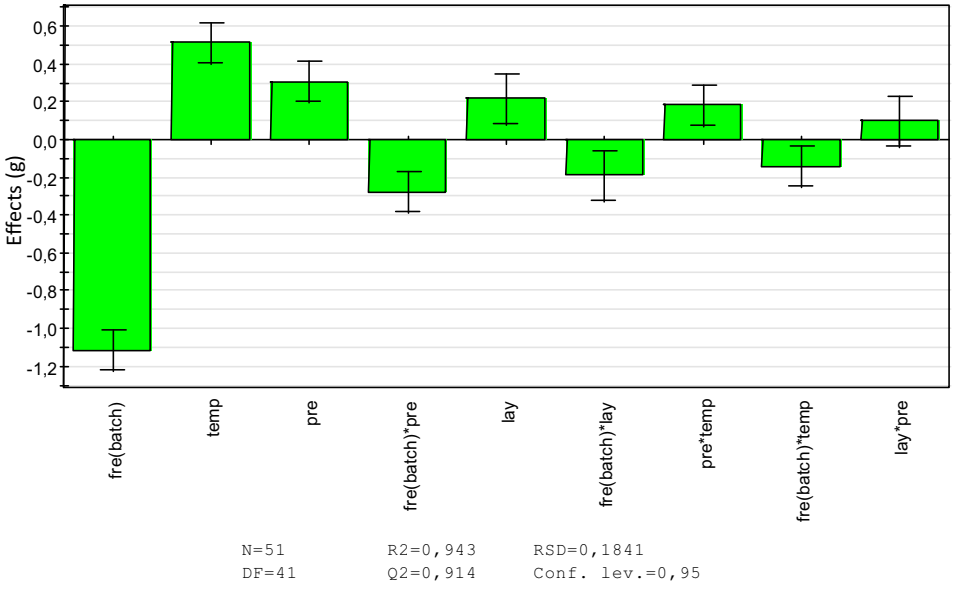


**Fig. 8.** Effect plot off the full factorial design for formulation 1. Freezing method (fre), temperature (temp), chamber pressure (pre), layer thickness (lay).

**Table 4**
overview of the coefficient plots.

| Factor | Level | Formulation 1 | Formulation 2 | Formulation 3 | Formulation 4 | Formulation 5 |
|---|---|---|---|---|---|---|
| Free | Spin | +++ | +++ | +++ | +++ | +++ |
| | Batch | – – – | – – – | – – – | – – – | – – – |
| Lay | | + | + | + | +* | + |
| Coo | LN2 | – | –* | – | +* | + |
| | Dry ice | + | +* | + | –* | – |
| Pre | | + | + | + | + | ++ |
| Temp | | ++ | ++ | ++ | ++ | ++ |

Freezing method (fre), temperature (temp), chamber pressure (pre), layer thickness (lay) , + small positive effect, ++ positive effect, +++ large positive effect, – small negative effect, – – – large negative effect.
* non-significant effect.

evaluated. The applied shelf temperature and filling volume were 40 °C and 3.5 ml, respectively. An overview of the design experiments is given in Table 3.

Both designs were developed and analyzed using the Modde 9.1.1.0. software (Umetrics AB, Umeå, Sweden).

For each effect plot, the number of experiments (N) and degrees of freedom (DF) are given. The following statistical parameters were calculated: i. *R*2 being the fraction of the variation of the response explained by the model; ii. *Q*2 being the fraction of the variation of the response predicted by the model according to cross

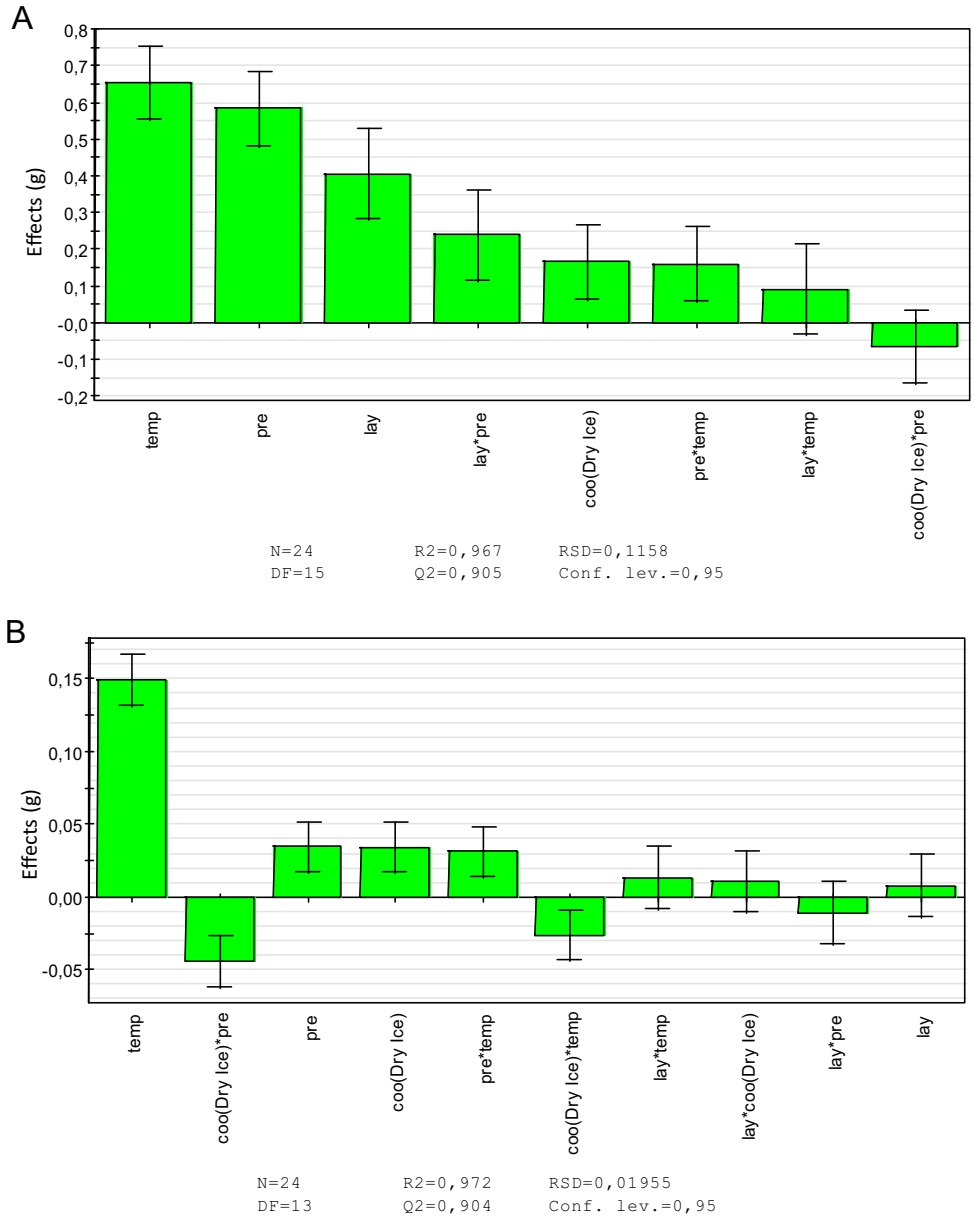


**Fig. 9.** (A) effect plot for formulation 1 split for freezing method: spin freezing temperature (temp), pressure (pre), layer thickness (lay), freezing rate (coo). (B) effect plot for formulation 1 split for freezing method: traditional batch freezing. temperature (temp), pressure (pre), layer thickness (lay), freezing rate (coo).

**Table 5**
overview of the coefficient plots for the split designs.

| Spin | | | | | | |
|---|---|---|---|---|---|---|
| Factor | Level | Formulation 1 | Formulation 2 | Formulation 3 | Formulation 4 | Formulation 5 |
| Lay | | ++ | ++ | ++ | ++ | ++ |
| Coo | LN2 | – | –* | –* | +* | +* |
| | Dry ice | + | +* | +* | –* | –* |
| Pre | | +++ | +++ | +++ | +++ | +++ |
| Temp | | +++ | +++ | +++ | +++ | +++ |

| Batch | | | | | | |
|---|---|---|---|---|---|---|
| Factor | Level | Formulation 1 | Formulation 2 | Formulation 3 | Formulation 4 | Formulation 5 |
| Lay | | +* | / | +* | +* | / |
| Coo | LN | – | / | – | / | +* |
| | Dry ice | + | / | + | / | –* |
| Pre | | + | + | + | +* | ++ |
| Temp | | ++ | +++ | ++ | ++ | +++ |

Temperature (temp), pressure (pre), layer thickness (lay), freezing rate (coo), / no effect, + small positive effect, ++ positive effect, +++ large positive effect, – small negative effect.
* non-significant effect.

validation; iii. The residual standard deviation (RSD) being computed using the total number of experiments

### 4.3. NIR equipment

To determine the endpoint of primary and secondary drying in spin frozen vials, an NIR probe coupled to a fourier-transform near infrared (FT NIR) spectrometer (Thermo Fisher Scientific, Zellik, Belgium, Nicolet Antaris II near-IR analyzer) was implemented in the freeze-dryer and placed in the vial holder (see Fig. 6).

The diffuse reflectance NIR spectra were collected in a continuous and non-invasive way during the in-line NIR experiments (see Section 5.2). The NIR spectrometer was equipped with an InGaAS detector, a quartz halogen lamp and a fiber-optic non-contact probe which was brought into the freeze-dryer chamber through a port in the sidewall. Spectra were taken from 10000 $cm^{-1}$ to 4500 $cm^{-1}$ with a resolution of 8 $cm^{-1}$ and averaged over 32 scans. Every process minute, a spectrum was recorded.

The NIR probe was positioned through a hole in a vial holder for the spin-frozen vials. The sidewall of the vial was hence monitored with a spot size of about 28 $mm^2$. The effective sample size measured by the NIR probe hence consisted of a small part of the total sample volume (3.5 ml) (see Fig. 6). It was from a practical point of view not possible and also not desired (since non-contact measurements are preferred) to bring a NIR probe inside the vial.

### 4.4. Multivariate data analysis

Principal component analysis (PCA) was applied to analyze the in-line collected NIR spectra using a multivariate data analysis software package (Simca 13.0.3, Umetrics AB, Umeå, Sweden). The spectra were preprocessed using standard normal variation (SNV) and mean centering prior to analysis.

PCA is a multivariate data analysis technique, also widely used for NIR spectroscopic process monitoring (Massart et al., 1997). PCA produces an orthogonal bilinear data matrix decomposition, where principal components (PCs) are obtained in a sequential

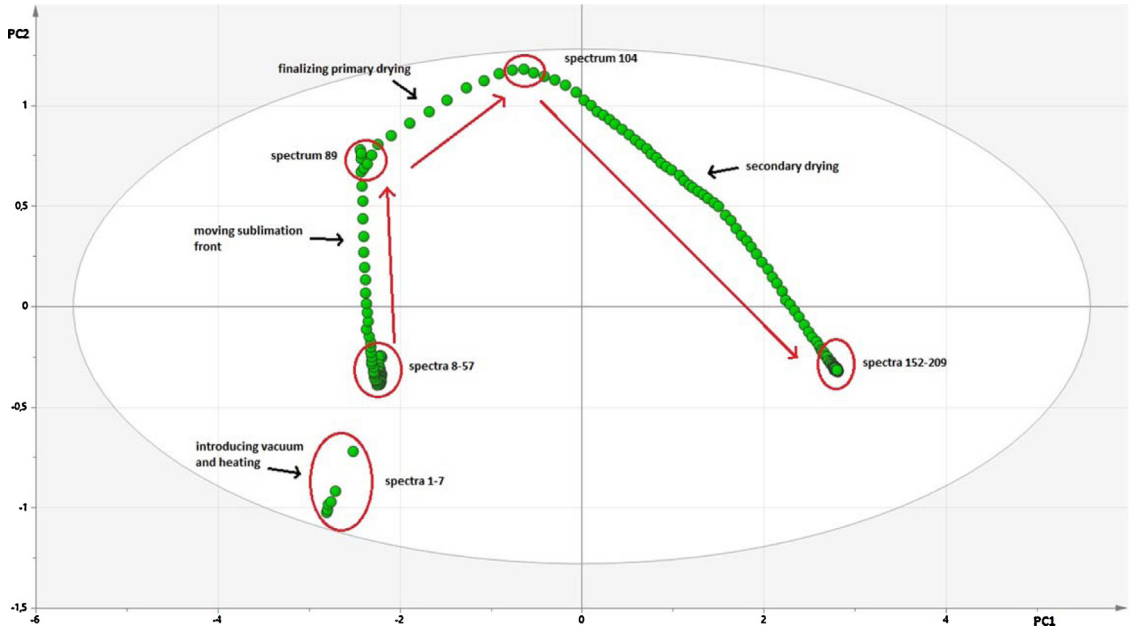


**Fig. 10.** PC1 versus PC2 scores plot obtained after PCA on in-line collected NIR spectra of formulation 1.

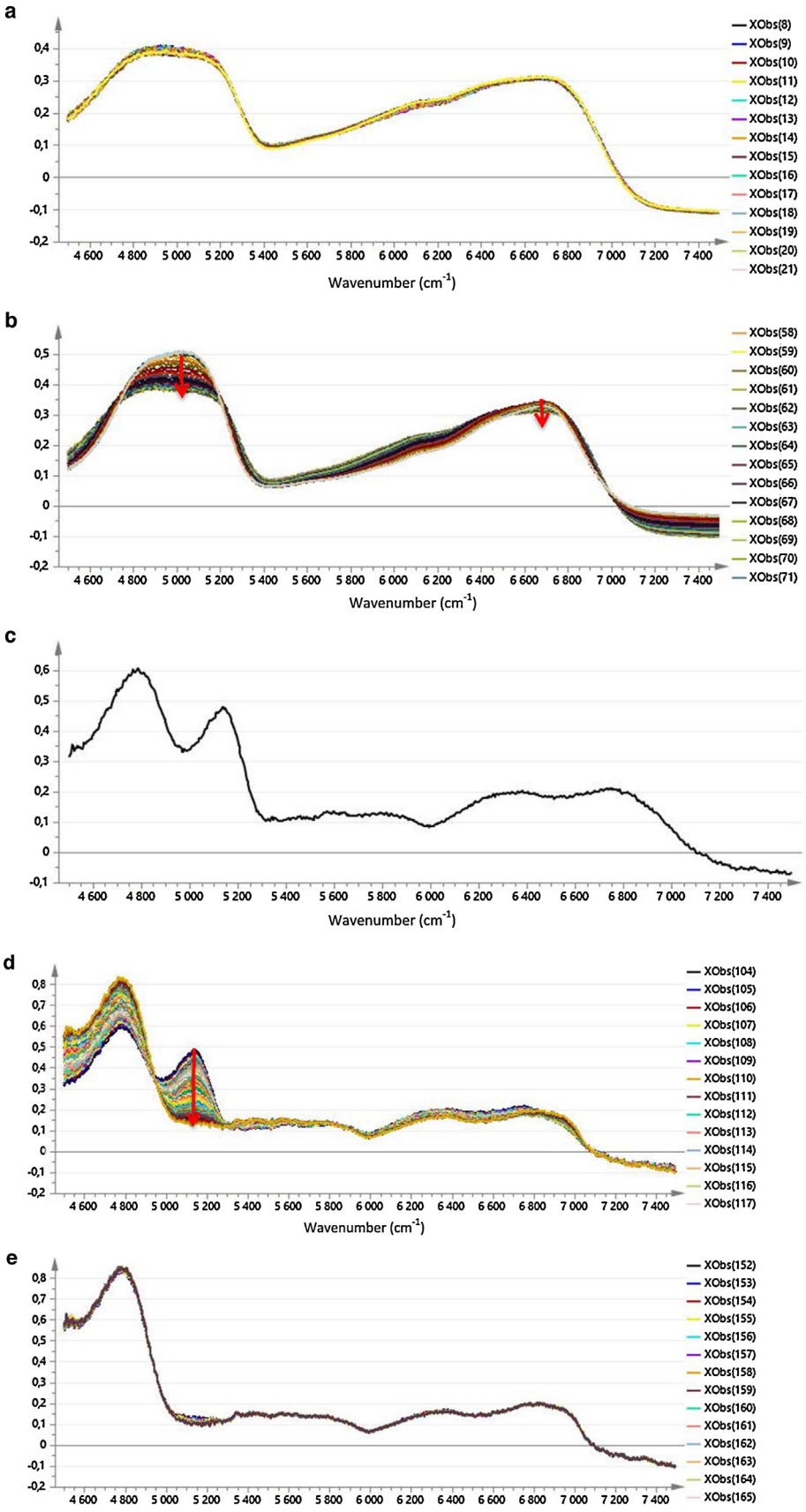


**Fig. 11.** (a) spectra 8–57. (b) spectra 58–88, underlying product signals appear in the spectrum. (c) spectrum 104, end of primary drying. (d) spectra 104–152, water band intensity at 5160 $cm^{-1}$ is decreasing during secondary drying (Pieters et al., 2012). (e) spectra 152–209, end of secondary drying.

way to explain maximum variance:

$$D = TP^{T} + E = t_1 p_1^{'} + t_2 p_2^{'} + \ldots + t_Q p_Q^{'} + E$$

where $T$ is the M × Q score matrix, $P$ the N × Q loading matrix, $E$ the M × N model residual matrix, $Q$ the number of PCs, $N$ the number of collected spectra at $M$ wavelengths. Each PC consists of two vectors, the score vector $t$ and the loading vector $p$. The score vector contains a score value for each spectrum, and this value informs how the spectrum is related to the other spectra in that particular component. The loading vector indicates which spectral features in the original spectra are captured by the component studied. These unique and orthogonal PCs can be very helpful in deducing the number of different sources of variation present in the data and the occurrence of groups of related objects. However, these PCs do not necessarily correspond to the true underlying factors causing the data variation, since each PC is obtained by maximizing the amount of remaining variance (De Beer et al., 2008)

## 5. Results and discussion

### 5.1. Spin freezing versus traditional freezing

Eq. (1) (Kuu et al., 2006; Overcashier et al., 1999), describing the sublimation rate during primary drying, clearly suggested a higher sublimation rate for spin frozen vials due to the higher surface area ($A$) and the thinner product layer (resulting in a less important $R_p$ parameter) of spin frozen vials compared to traditional frozen vials.

$$\frac{dm}{dt} = \frac{A}{R_p}(P_p - P_c) \quad (1)$$

where $dm/dt$ is the sublimation rate (g/h), $A$ is the surface area of the frozen product layer ($cm^2$), $R_p$ is the area-normalized dried product resistance ($cm^2\,m\,Torr\,h\,g^{-1}$). $P_p$ is the equilibrium vapor pressure of ice at the temperature of the sublimating ice (m Torr) and $P_c$ is the chamber pressure (m Torr). In our spin frozen vials, the frozen product surface area was 6.8 times higher and the dried product resistance is lower due to the thin layer (1.2–1.7 mm, depending on the applied volume in our experiments) compared to traditional frozen vials (8–10.7 mm).

After having performed its experiments, design 1 (see Section 4.2) was analysed using the Modde software. The effect plot in Fig. 7 showed the largest effect for the factor 'freezing method (fre)' upon the amount of sublimated water after 2 h of drying. Batch freezing clearly had a negative significant effect upon the response. This confirmed the hypothesis that spin frozen vials have much higher sublimation rates compared to traditional frozen vials due to the larger surface area and the thinner product layer of the spin frozen vials.

Changing the factor 'shelf temperature (temp)' from 5 °C to 40 °C whilst keeping the other factors at their center point increased the mass of sublimated water after 2 h by 0.57 g (Fig. 7). Increasing the shelf temperature resulted in a higher energy supply towards the frozen product and thus a faster sublimation.

The factor 'chamber pressure (pre)' had an effect of 0.41 g. Increasing the chamber pressure meaned that more gas molecules were present in the space between the vial and the shelf or vial holder. The convective heat transfer became then more efficient, leading to a faster sublimation (Ganguly et al., 2013).

'Freezing rate (coo)' had no significant effect on the mass of sublimated water after 2 h drying, suggesting that both freezing rates (liquid nitrogen versus dry ice) did not lead to relevant different degrees of supercooling. The higher the degree of supercooling, the higher the amount of small ice crystals. Small ice crystals have a large surface area, hence leading to a lower sublimation rate and a faster desorption compared to a low degree of supercooling which results in larger ice crystals (Kasper and Friess, 2011). The effect of supercooling during spin freezing will be examined in further research. It was expected that the spinning may trigger the ice nucleation leading to similar degrees of supercooling when using different freezing rates, which could explain the factor 'freezing rate' not being significant in this study.

The effect of 'filling volume (lay)' upon the mass of sublimated water is low (0.23 g). The filling volume was related to the product layer thickness (Table 2). Since after 2 h of primary drying only the top layer of the frozen product was sublimated in both the spin frozen vials and the traditional frozen vials, it could be indeed expected that the factor filling volume is less relevant. The dry product resistance only increased with higher dry product layer thicknesses. The effect is not non-significant since the product surface area in spin-frozen (2533 $mm^2$) and traditionally frozen (373 $mm^2$) vials was different. For the factor 'formulation (pro)', formulation 1 showed a negative effect. The slower sublimation rate could be explained by the higher solutes concentration compared to the other formulations. Formulation 5, containing only sucrose shows a positive significant effect. It was unclear why this formulation had a faster sublimation rate compared to the other four formulations, although having the second highest $R_p$ value.

In a next step, this design (design 1) was divided into 5 subdesigns, i.e., one full factorial design for each formulation, allowing a more detailed analysis of the influence of the other examined factors upon sublimation rate per formulation. This subdivision did not require performing new experiments. Each subdesign was a full factorial design consisting of one factor with three levels and four factors each with two levels (Table 2), resulting in 48 experiments.

Similar effects could be observed for each formulation (i.e., each subdesign). The effect plot of the subdesign from formulation 1 is shown in Fig. 8. An overview of the effects for the other formulations (i.e., the other sub designs) is given in Table 4.

The factor 'freezing method (fre)' has in all five designs the largest effect. This confirmed again that spin freezing resulted in much higher sublimation rates. Chamber pressure (pre), shelf temperature (temp) and filling volume (lay) had similar positive effects for all formulations (see explanation overall design higher).

**Table 6**
overview of conclusions obtained after analysis of the NIR spectra.

| | 100 μbar | | 300 μbar | |
|---|---|---|---|---|
| | 1° drying endpoint (min) | 2° drying endpoint (min) | 1° drying endpoint (min) | 2° drying endpoint (min) |
| Formulation 1 | 103 | 152 | 80 | 138 |
| Formulation 2 | 124 | 158 | 103 | 139 |
| Formulation 3 | 134 | 157 | 105 | 133 |
| Formulation 4 | 108 | 174 | 103 | 152 |
| Formulation 5 | 114 | 153 | 88 | 146 |

In a final step, the above described 5 subdesigns were further subdivided according to freezing method, resulting in a total of ten full factorial designs. This subdivision did not require performing new experiments. Hence, in each subdesign, corresponding to 1 formulation and a specific freezing method, the influence of layer thickness, freezing rate, shelf temperature and chamber pressure upon mass of water sublimed after 2 h drying was studied.

The analysis of the effects of the full factorial designs for formulation 1 for both freezing methods is shown in Fig. 9A (spin freezing) and B (traditional freezing). An overview of the effects for the other formulations is given in Table 5. The major difference between the effect plots for spin frozen vials and traditional frozen vials was the effect of the chamber pressure. For spin frozen vials, the effect of chamber pressure and temperature was within the same range: 0.65 g and 0.58 g sublimated water after 2 h drying, respectively (see Fig. 9A). However, chamber pressure was expected not to be significant for the spin frozen vials when having optimal direct contact between vial holder and vial. The importance of chamber pressure hence indicated inadequate contact between vial and vial holder. An increased chamber pressure then resulted in more gas molecules between the vial and the shelf or vial holder, leading to more efficient convective heat transfer, resulting in a faster sublimation.

For traditional frozen vials, the effect of chamber pressure (0.034 g) was much smaller compared to shelf temperature (0.149 g) (see Fig. 9B), since the product-vial surface area was much smaller compared to spin frozen vials (373 $mm^2$ versus 2533 $mm^2$).

The largest effect for spin frozen vials and traditionally frozen vials is shelf temperature. The quantitative value of this effect was 0.65 g and 0.15 g sublimated water, respectively. The higher quantitative value for spin frozen vials could be explained by the faster sublimation rate of spin frozen vials (see higher).

Layer thickness had a positive and significant effect for spin-frozen formulation 1 (0.41 g). A similar result could be found for the other four spin frozen formulations. This result could not be explained as mentioned above.

The rationale for creating and analyzing these subdesigns was to distinguish the effect of the factors for each formulation independently. This became for example clear for the shelf temperature and chamber pressure effects. In the overall design, these effects were 0.13 g and 0.08 g, respectively. In the subdesigns, after splitting for formulation and freezing method, the effects of shelf temperature and chamber pressure were 0.65 g and 0.58 g for spin frozen vials but 0.15 g and 0.03 g for traditional frozen vials.

### 5.2. In-line NIR monitoring of the freeze-drying process.

Fig. 10 shows the PC 1 versus PC 2 scores plot obtained after principal component analysis (PCA) of the in-line collected NIR spectra of experiment 1 (design 2, see materials and methods).

During the first seven drying minutes, the vacuum was introduced and the temperature of the shelves and vial holder increased. This could be seen in the scores plot as the scores move towards the first cluster (spectra 1–7). From 8 to 57 min, ice sublimation occurred but is not visible in the NIR spectra since ice sublimation started on the top (inner side wall) of the frozen layer while NIR spectra were collected from the outer sidewall of the vials. The penetration depth of the NIR light was not sufficient to detect the sublimation at the top of the product. Hence, no spectral changes were seen between 8 and 57 min (Fig. 11a) and the corresponding scores were clustered.

Between 58 min and 89 min, the intensity of the ice peaks around 5000 $cm^{-1}$ and 6700 $cm^{-1}$ started lowering and other product signals appeared in the spectrum (Fig. 11b). This could be explained by the fact that the sublimation front was moving towards the NIR probe at the outer wall of the vial. Spectral signals from the formulation became visible because of the decreasing amount of overwhelming ice signals. Spectrum 104 was the endpoint of primary drying since all ice signals had disappeared in this spectrum (Fig. 11c). Secondary drying started already after 89 min. During secondary drying the free water band at 5160 $cm^{-1}$ decreases in intensity (Fig. 11d) (Pieters et al., 2012; De Beer et al., 2009).

152 min after the start of the process, secondary drying was finished. The spectra from 152 min to 209 min formed a cluster, indicating that no changes occurred anymore in the product (Figure 11e).

This spectral analysis was done for the five formulations at the two different applied chamber pressure conditions. An overview of these PCA results is given in Table 6.

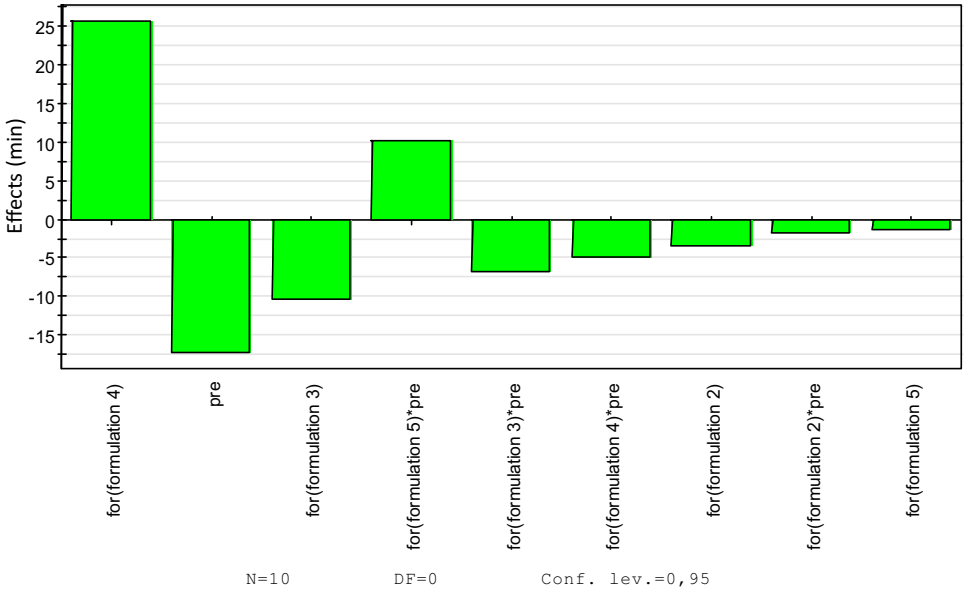


**Fig. 12.** Effect plot of the full factorial design for the in-line NIR monitoring formulation (for), pressure (pre).

The results of the full factorial design analysis is shown in Fig. 12. The effect of the factor chamber pressure upon drying time was negative. When this factor was changed from its lowest to its highest value whilst the other factors were kept at their center-point, resulted in a shorter drying time of 17 min. This result confirmed that a higher chamber pressure resulted in a shorter drying time. The explanation of this unexpected effect is given in Section 5.1.

Formulation 4 had a positive effect of 25 min. This result was contradictory to the results of Section 5.1 where formulation 4 had no significant effect on the response mass of sublimated water. A possible explanation was the formation of a dense lactose layer on the top of the dry product layer leading to a higher dry product resistance and thus a longer drying time (Chen et al., 2008).

## 6. Conclusion and future perspectives

Spin freezing as part of a continuous freeze drying concept for unit doses has been presented and evaluated. The sublimation rate in spin frozen vials is significantly higher compared to traditionally frozen vials. This can be explained by the larger product surface, and the lower importance of product resistance because of the much thinner product layers in the spin frozen vials compared to the traditionally frozen vials. Both chamber pressure and shelf temperature have a positive effect on the sublimation rate. For the experimental conditions tested in this study, the effect of chamber pressure is more important in spin frozen vials compared to traditionally frozen vials. The reason for this effect is the poor contact between the vial and the vial holder. An increased chamber pressure then results in more gas molecules between the vial and the shelf or vial holder, leading to more efficient convective heat transfer, resulting in a faster sublimation. Due to the larger product-vial surface area of the spin frozen vials, this factor has a large impact on the sublimation rate.

In-line NIR monitoring of spin frozen vials allowed monitoring the entire drying process and determining the primary and secondary drying endpoints, and confirmed the effect of chamber pressure on the total drying time.

Mathematical modeling and simulation of the drying process for the five used model formulations, allowing further clarification of the experimental observations, will be extensively described in a next manuscript.

## References


Baertschi S.W., Alsante K., Reed R., 2011 Pharmaceutical stress testing: prediction drug degradation, second edition, CRC Press.

Chen, R., Slater, N.K., Gatlin, L.A., Kramer, T., Shalaev, E.Y., 2008. Comparative rates of freeze-drying for lactose and sucrose solutions as measured by photographic recording, product temperature and heat flux transducer. Pharm. Dev. Technol. 13 (5), 367–374.

J.A.W.M. Corver 2013. Method and system for freeze-drying injectable compositions, in particular pharmaceutical. WO2013036107.

De Beer, T., Vercruysse, P., Burggraeve, A., Quinten, T., Ouyang, J., Zhang, X., Vervaet, C., Remon, J.P., Baeyens, W.R.G., 2008. In-line and real-time process monitoring of a freeze drying process using raman and NIR spectroscopy as complementary process analytical technology (PAT) tools. J. Pharm. Sci. 98 (9), 3430–3446.

De Beer, T., Wiggenhorn, M., Veillon, R., Debacq, C., Mayeresse, Y., Moreau, B., Burggraeve, A., Quinten, T., Friess, W., Winter, G., Vervaet, C., Remon, J.P., Baeyens, W.R.G., 2009. Importance of using complementary process analyzers for the process monitoring, analysis and understanding of freeze drying. Anal. Chem. 81 (18), 7639–7649.

Ganguly, A., Nail, S.L., Alexeenko, A., 2013. Experimental determination of the key heat transfer mechanisms in pharmaceutical freeze-drying. J. Pharm. Sci. 102 (5), 1610–1625.

ICH Q8(R2), 2009; US FDA. PAT guideline, 2004.

Kasper, J.C., Friess, W., 2011. The freezing step in lyophilisation: physico-chemical fundamentals, freezing methods and consequences on process performance and quality attributes of biopharmaceuticals. Eur. J. Pharm. Biopharm. 78, 248–263.

Kauppinnen, A., Toiviainen, M., Korhonen, O., Aaltonen, J., Järvinen, K., Paaso, J., Juuti, M., Ketolainen, J., 2013. In-line multipint near-infrared spectroscopy for moisture content quantification during freeze-drying. Anal. Chem. 85 (4), 2377–2384.

Khairnar, S., Kini, R., Harwalkar, M., Salunkhe, K., Chaudhari, S.R., 2013. A review on freeze drying process of pharmaceuticals. Int. J. Res. Pharm. Sc. 4 (1), 76–94.

Kuu, W.Y., Hardwick, L.M., Akers, M.J., 2006. Rapid determination of dry layer mass transfer resistance for various pharmaceutical formulations during primary drying using product temperature profiles. Int. J. Pharm. 313, 99–113.

Massart, D.L., Vandeginste, B.G.M., Buydens, L.M.C., De Jong, S., Lewi, P.J., Smeyers-Verbeke, J., 1997. Handbook of Chemometrics and Qualimetrics: Part A. Amsterdam, Elsevier.

Overcashier, D.E., Patapoff, T.W., Hsu, C.C., 1999. Lyophilization of protein formulations in vials: investigation of the relationship between resistance to vapour flow during primary drying and small-scale product collapse. Eur. J. Pharm. Sci. 88.

Pieters, S., De Beer, T., Kasper, J.C., Boulpaep, D., Waszkiewicz, O., Goodarzi, M., Tistaert, C., Friess, W., Remon, J.-P., Vervaet, C., 2012. Near-infrared spectroscopy for in-line monitoring of protein unfolding and its interactions with lyoprotectants during freeze-drying. Anal. Chem. 84, 947–955.

Pikal, M.J., 2002. Encyclopedia of Pharmaceutical Technology. Marcel Dekker, New York, pp. 1299–1326.

Rambhatla, S., Ramot, R., Bhugra, C., Pikal, M.J., 2004. AAPS Pharm. Sci. Tech. 5 (4) Article 58.

Ramsay B.G., 2003. Vacuum chamber load lock structure and article transport mechanism. US6609877.

Tang, X., Pikal, M.J., 2004. Design of freeze-drying processes for pharmaceuticals: practical advice. Pharm. Res. 21 (2), 191–200.

Trappler, E.H., 2004. Encyclopedia of Pharmaceutical Technology. Marcel Dekker, New York, pp. 1–18.

Wang, W., 2000. Lyophilization and development of solid protein pharmaceuticals. Int. J. Pharm. 203 (2000), 1–6.